Regional Climate Variability Impacts on the Annual Grape Yield in Mendoza, Argentina

Eduardo Agosta and Pablo Canziani

Equipo Interdisciplinario para el Estudio de Procesos Atmosféricos en el Cambio Global, Pontificia Universidad Católica Argentina, and Consejo Nacional de Investigaciones Científicas y Técnicas, Buenos Aires, Argentina

Martín Cavagnaro

Equipo Interdisciplinario para el Estudio de Procesos Atmosféricos en el Cambio Global, Buenos Aires, and Facultad Regional Mendoza, Universidad Tecnológica Nacional, Mendoza, Argentina

ABSTRACT

Mendoza Province is the major Argentinian vitivinicultural region, and its grape production is fundamental for the national vintage. The 1979–2009 climate–annual grape yield relationships are analyzed, and total grape yield is shown to depend significantly on regional "summer" (October–March) precipitation. Precipitation negatively affects yields through plant disease and damage/destruction by hail. At interannual scales, summer regional precipitation variability can explain 25% of the yield variance. Summer precipitation modulates yield with a 6–8-yr period: wet (dry) summers can be associated with larger (smaller) grape damage/loss probability during the summer preceding the vintage, as well as lower (higher) grape yields in the subsequent annual campaign because of bud damage. With respect to monthly mean precipitation at Mendoza Observatory, wetter Novembers/Decembers can lead to lower yields. Hail during the summer of the previous harvest and during December could lower yields. Winter, late spring, and early summer mean maximum temperatures can impact current and subsequent annual yields: warmer (colder) months are linked to enhanced (decreased) yields. These relationships can be associated with circulation and SST conditions in the equatorial and extratropical Pacific Ocean basin and southern South America: SSTs within the southeastern South Pacific are related to western equatorial Pacific SSTs and convection, which modify circulation and water vapor transport over southern South America. Statistical multilinear modeling shows that the observed relationships among yield, precipitation, and temperature can explain at least 60% of the observed interannual yield variability. It is thus possible to quantitatively estimate, some months in advance, the upcoming vintage's yield.

1. Introduction

The climate in central-western Argentina (CWA), between 28° and 36°S and between 65° and 70°W (Fig. 1), known as the Cuyo region, is arid to semiarid, under the rain shadow of the high western Andes mountains, whose peaks reach between 5000 and 6000 m above mean sea level on average. The mean lower-tropospheric circulation is characterized by the interaction between moist and warm northeasterly winds from the quasi-stationary subtropical South Atlantic anticyclone (SAA), centered at about 30°S over the South Atlantic Ocean basin, the continental thermal–orographic–dynamic *chaco* low, and the westerlies at higher latitudes (Agosta and Compagnucci 2012). Such a climate favors grape production under irrigation to such an extent that this is the main grape-growing region in Argentina, and grape production and industrialization are major components of the regional economy. Within Cuyo, Mendoza Province carries nearly 70% of the national vineyard area, with over 65% of the total national grape production. Hence, the province leads the national wine agribusiness in production of both total grapes and wine [Instituto Nacional de Vitivinicultura (INV); online at http://www.inv.org.ar].

Agosta and Cavagnaro (2010) recently found that total grape yield variability is partly related to summer

Corresponding author address: Eduardo Andres Agosta, PEPACG, Pontificia Universidad Católica, Edificio San José, Av. A. Moreno de Justo 1600, 3er piso, Puerto Madero C1107AAZ, Buenos Aires, Argentina.
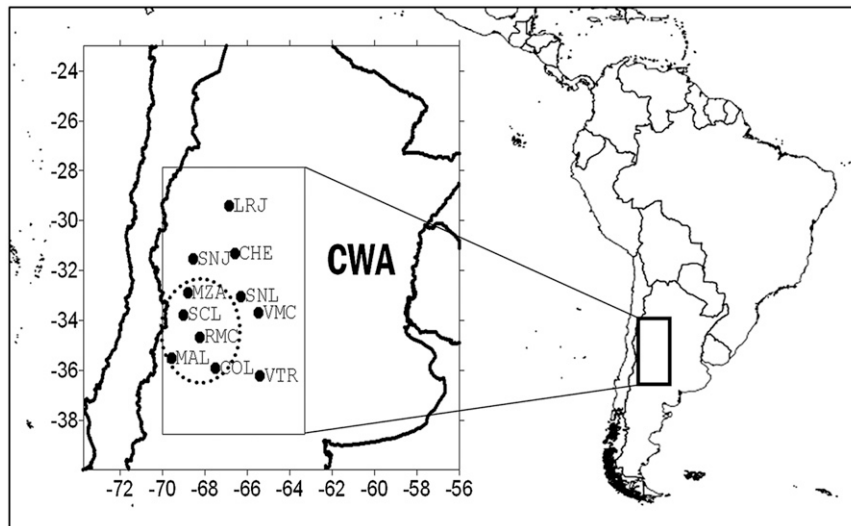E-mail: eduardo.agosta@conicet.gov.ar

FIG. 1. Map of the CWA region showing the location of the operational weather surface stations the data of which are used in this study; see Table 1 for the station list and geographic coordinates. A dashed line encircles the meteorological stations within Mendoza Province.

(October–March) precipitation interannual variability in CWA. The CWA summer precipitation variability shows interannual to multidecadal variability throughout the past century, with prominent low-frequency quasi cycles (Compagnucci et al. 2002; Agosta and Compagnucci 2012). The quasi-bidecadal oscillation with a period of about 18 yr is a strong feature of the CWA summer precipitation; it resulted in alternating wet and dry spells, lasting approximately 9 yr each, until the 1970s. Since then, the CWA region has undergone a prolonged wet spell that has lasted more than 30 yr. The loss of the quasi-bidecadal signal in precipitation can be attributed to impacts on the regional atmospheric circulation resulting from the 1976/77 climate transition (Agosta and Compagnucci 2008a). This climate transition is linked to warmer sea surface temperature anomalies in the central Pacific Ocean (Mantua et al. 1997; Alexander 2010). Grape yield records, however, are available in Mendoza only since 1979, corresponding to the long-term wet period in CWA.

In the current climate change context (Solomon et al. 2007; Parry et al. 2007), in which adaptation strategies need to be designed to ensure the continuity of the activity [e.g., Organization Internationale de la Vigne et du Vin (OIV) Strategic Plan; see online at http://www.oiv.int], the analysis of the temporal evolution of Mendoza's grape production with respect to current regional climate variability can provide research-supported baseline information for decision-making processes at medium and long-term scales. Studies such as Jones and Davis (2000), Jones et al. (2005), Grifoni et al. (2006), Hall and Jones (2008, 2010), and Makra et al. (2009) have looked at climate–production relationships for grape- and wine-producing regions in Australia, Europe, and North America. Very few studies have analyzed these issues for South American production, however. In the case of Argentine vitivinicultural regions, Barbero et al. (2008) have looked at the regional climate evolution and associated changes in phenological indicators since the early 1970s for northern and central Patagonia, where there is a growing grape and wine industry. They also considered future implications using regional climate model runs with Intergovernmental Panel on Climate Change scenarios for 2070–80.

The aim of this study is to examine in detail the relationship between the CWA interannual climate variability, as given by precipitation and temperature, and Mendoza's total grape production for the period 1979–2009. Mendoza's vintage takes place most commonly in April. It would be possible in principle, by determining the relative contributions of these climate variables, to quantitatively estimate the impact of regional climate on the province's annual grape yields. Section 2 introduces the datasets used in the study, both direct observations and reanalysis products, as well as statistical and atmospheric dynamics diagnostics tools applied. Section 3 introduces first the overall relationship between summer precipitation in Cuyo and annual grape yield. A low-frequency variability analysis is subsequently carried out to further understand the observed precipitation–grape yield relationships. Monthly precipitation and temperature retrievals are then considered to understand these relationships within the grape

growth cycle. A climate dynamics diagnostic is then applied to determine possible circulation mechanisms driving the observed variability and statistical relationships. A backward-stepwise model is then used to define the main climate predictors that can be used to explain the grape yield variability. A three-variable model is obtained that optimizes yield prediction by early December. This analysis shows that it is possible to use regional South Pacific SSTs from August, precipitation from January of the summer of the previous harvest, and the November maximum temperature of the current growth cycle to reach such a prediction.

2. Data and method

The required grape production data are provided by the INV statistics office, that is, Mendoza's total annual grape production in metric quintals (100 kg) and total implanted surface area, in hectares, for the period 1979–2009. These statistics are used to estimate the annual total grape yield (or, simply, yield) as the ratio of the total grape production to the total implanted area. Meteorological data from 11 stations operated by the Servicio Meteorológico Nacional in the Cuyo region (Table 1) are used. Monthly mean maximum and minimum temperatures and total monthly precipitation data are considered in this study. In addition, the total vineyard area damaged by hail (SDG), in hectares, in Mendoza Province, as surveyed by the Dirección de Agricultura y Contingencias Climáticas (http://www.contingencias.mendoza.gov.ar), is also considered for the summers between 1994 and 2006 according to availability.

The precipitation's interannual variability during summer (defined here as the warm season extending from October through March, that is, equivalent to the Southern Hemisphere grape-growing season) has been studied in detail by Agosta et al. (1999) and Compagnucci et al. (2002). They established an annual regional index (CWAP) for summer precipitation in CWA that is used in this study. The CWAP index is calculated as the seasonal percentage ratio of the precipitation with respect to the sampled period's mean averaged for all stations available each year and subsequently standardized. First, an intermediate $P(t)$ index is estimated as the percentage ratio between total (October–March) summer rainfall at each station and the station mean, averaged over all of the stations:

$$Y_j(t) = [X_j(t) \times 100]/\chi_j, \quad 1 \le j \le n, \qquad (1)$$

where $Y_j(t)$ is the summer rainfall annual series for station j, given as a percentage of its 1961–90 long-run

TABLE 1. Meteorological stations that are used for the construction of CWAP (Fig. 1).

Station	Height (m)	Lat (°S)	Lon (°W)	Record length
La Rioja (LRJ)	516	29.42	66.87	1904–2010
San Juan (SNJ)	634	31.32	68.57	1900–2010
Chepes (CHE)	658	31.33	66.60	1930–90
Mendoza (MZA)	769	32.88	68.82	1900–2010
San Luis (SNL)	734	33.03	66.32	1905–2010
Villa Mercedes (VMC)	514	33.68	65.48	1900–2010
San Carlos (SCR)	940	33.77	69.01	1938–79
Rama Caída (RMC)	713	34.67	68.40	1927–2010
Colonia (COL)	465	35.00	67.69	1935–79
Malargüe (MAL)	1425	35.50	69.58	1953–2010
Victorica (VTR)	312	36.23	65.43	1905–2010

average χ_j, corresponding to the October–March warm period, and n is the total number of stations considered (11 in this study).

Hence,

$$P(t) = \sum_{j=1}^{n} Y_j(t)/n \quad \text{and} \qquad (2)$$

$$\text{CWAP}(t) = \frac{P(t) - \overline{P(t)}}{\sigma[P(t)]}, \qquad (3)$$

where $\overline{P(t)}$ is the $P(t)$ time mean over the period sampled and $\sigma[P(t)]$ is the $P(t)$ standard deviation. Thus, a positive (negative) CWAP index signals a wet (dry) summer in Cuyo. Because summer precipitation in CWA is frequently convective and accompanied by hailstorms (Saluzzi 1992), here a wet (dry) summer implies more (less) precipitation, which can be due to rain, hail, or both, as will be discussed. The CWAP index is used here to analyze CWA summer precipitation variability and the relationship with Mendoza's annual yield.

To study the interannual relationship between yield and both local precipitation and temperature within the annual cycle, monthly total precipitation (PPP) and monthly mean maximum and minimum temperatures (T_{max} and T_{min}, respectively) for the Mendoza Observatory weather station (MZA; Table 1) are used. In particular, MZA is used as a reference for the interannual monthly comparison between yield and temperature/precipitation. This choice was made for the following reasons: 1) the station's long, almost gapless data record with very good quality observations and 2) the station's closeness to the Eastern Zone oasis, which remains the most important grape-growing region within the province, with nearly 50% of the province's grape yield.

Monthly mean atmospheric and oceanic variables required for the analysis, such as precipitable water

(PRWTR; kg m^{-2}), streamfunction (PSI; m^2 s^{-1}) at sigma levels 0.85 and 0.21, surface temperature (AIR; K), outgoing longwave radiation (OLR; W m^{-2}), and surface skin temperature [monthly Reynolds's sea surface temperature (SST); K] are obtained from the National Centers for Environmental Prediction–National Center for Atmospheric Research (NCEP–NCAR; Kistler et al. 2001) reanalysis dataset, available from the National Climatic Data Center (online at http://www.ncdc.noaa. gov). These data are provided at pressure levels on a 2.5° × 2.5° latitude–longitude grid. Reanalysis data at sigma levels are provided in a triangular spectral T62 Gaussian grid (192 × 94).

Correlation and regression maps between the yield in Mendoza and PRWTR, PSI, AIR, OLR, and SST are estimated to identify possible large-scale circulation patterns over southern South America and the Southern Hemisphere that can have an impact on the yield. Statistical time series analysis is carried out using multiple-regression analysis between grape production, as given by the yield, and the precipitation index (CWAP) for the current year's harvest (lag = 0) and the previous one (lag = −1). To isolate different time scales of variability and to examine the changes of variance in both the yield and CWAP time series, the complex Morlet wavelet transform is used to estimate wavelet power spectra for each time series. Further details on wavelet analysis can be found in Torrence and Compo (1998). To reduce edge effects, each time series is padded with zeros. To identify the frequency bands within which yield and CWAP time series are covarying, the cross-wavelet power spectrum is used (Torrence and Webster 1999). Wavelet coherence is also estimated as a measure of the intensity of the covariance of the two time series in time–frequency space, since cross-wavelet power is a measure of common power (Jevrejeva et al. 2003, 2005). A Markovian red-noise process (lag 1) is used to identified significant variances at $\alpha = 0.05$. The CWAP time series was smoothed using a nine-term Gaussian low-cut filter to highlight interdecadal variability of perturbations with periods over 9 yr. Last, a backward-stepwise multiple regression between grape yield and selected climate variables is applied to identify the best predictive model for the annual grape yield.

To diagnose the observed quasi-stationary wave activity observed in the climatological analysis in section 3d, the Plumb quasi-stationary wave activity flux (Plumb 1985) is calculated. Flux calculations provide information about wave sources and sinks necessary to understand the dynamics of the processes under study. For small-amplitude waves on a zonal mean flow, the conservative relationship for stationary wave activity is given by flux $\mathbf{F}_s$, which in this particular case is introduced only on the horizontal plane:

$$\mathbf{F}_s = p\cos\varphi\left[\overline{v}^{*2} - \frac{1}{2\Omega a \sin2\varphi}\frac{\partial(\overline{v^*\overline{\phi}^*})}{\partial\lambda}, \quad -\overline{u}^*\overline{v}^* - \frac{1}{2\Omega a \sin2\varphi}\frac{\partial(\overline{u}^{*2}\overline{\phi}^{*2})}{\partial\lambda}\right], \tag{4}$$

where p is the pressure; u^* and v^* are the eddy zonal and meridional geostrophic wind components, respectively; a is the earth's radius; ϕ is the geopotential; and $2\Omega\sin\varphi$ is the Coriolis parameter, with Ω being the earth's rotation rate and φ being latitude. In addition, overbars represent a time average and the quantities with asterisks denote departures from the zonal average. Flux $\mathbf{F}_s$ is parallel to the wave's group velocity.

3. Results

a. Annual grape yield and summer precipitation in Cuyo

Figure 2 shows the CWAP index (vertical bars) for the period 1901–2010, with respect to the 1979–2010 baseline. The smoothed curve, using a nine-term Gaussian filter (curve with triangles), is also shown to highlight the bidecadal quasi cycle that was present through the mid-1970s according to Compagnucci et al. (2002).

Figure 2 shows that since then, over the period under study, the state of the regional climate essentially is a long-lasting wet period. Agosta and Compagnucci (2008a) have shown that the CWA summer precipitation variability change, which took place in the mid-1970s, is associated with regional atmospheric circulation changes over southern South America, linked to the El Niño–like variability phase change that was observed in 1976/77 (Ebbesmeyer et al. 1991; Zhang et al. 1997; Mantua et al. 1997; Huang et al. 2005). It is well established that the El Niño–like variability, also known as Pacific decadal oscillation (PDO; Mantua et al. 1997) results in associated SST spatial structure changes approximately every 20–30 yr (Bond et al. 2003; Alexander 2010). This periodicity would appear to be absent in CWAP. Agosta and Compagnucci (2012) have recently shown that the CWA precipitation shift of 1976/77 is linked to Southern Hemisphere atmospheric circulation teleconnection changes associated with regional stationary anomalies found over the midlatitude southwestern
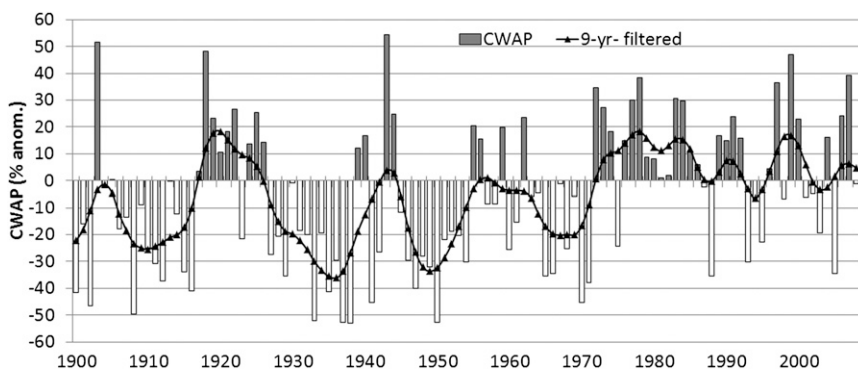
FIG. 2. CWAP summer precipitation index for CWA (vertical bars) together with the CWAP index smoothed with nine low-pass terms (CWAP FTR; line with squares), to emphasize the quasi-bidecadal cycle present until the mid-1970s.

South Atlantic (Agosta and Compagnucci 2008b). Pacific SST changes and other climate perturbations in the late 1990s suggest another reversal in the PDO phase (Bond et al. 2003; Grassi et al. 2012). The lack of a comprehensive mechanism explaining the El Niño–like variability and its persistence over extended periods, however, makes it impossible to determine true PDO reversals soon after they occur (Huang et al. 2005; Alexander 2010). Note that CWAP (Fig. 2) shows a slight decline after the early 2000s that may suggest, as yet inconclusively, a possible end to the prolonged wet period that started in the mid-1970s (Agosta and Compagnucci 2012).

Figure 3 shows yield and CWAP for 1979–2009. Yield exhibits a positive trend with a 0.40 correlation (98% significant). Part of this positive trend can probably be attributed to improvements in vineyard and strain selection practices, implemented in recent decades. Precipitation in the Cuyo region, on the other hand, shows an overall negative trend, with a weakly significant correlation of -0.20. Between 1979 and 1993 positive CWAP values were more frequent, but, as noted above, negative values have now become a somewhat more frequent occurrence: despite positive CWAP values in 2007 and 2008, the overall trend remains negative for the latter part of the sample.

Since only the time series' stationary components are relevant for examining the year-to-year CWAP and yield covariability, both time series are detrended. The unlagged correlation (lag = 0) between detrended CWAP and yield time series is -0.35, significant at the 95% confidence level. With a negative lag (lag $= -1$)— that is, correlating yield with respect to the summer precipitation of the previous year—the correlation is
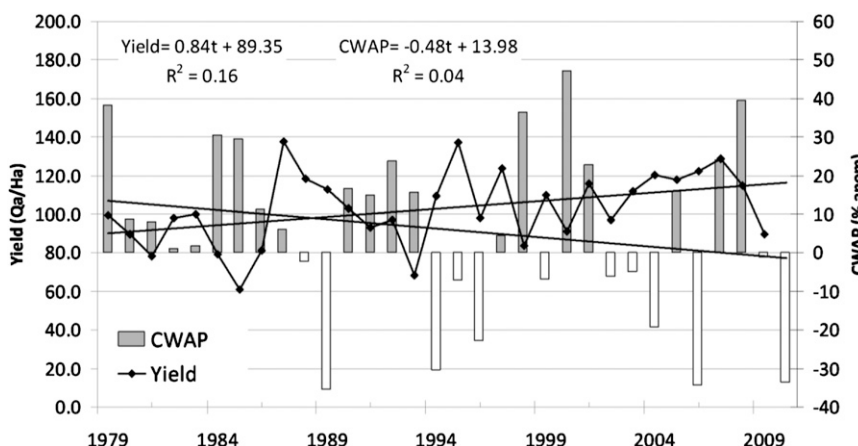

FIG. 3. Annual grape yield in Mendoza (metric quintals per hectare) ("Yield"; line with squares), together with CWAP summer precipitation index (vertical bars). The corresponding linear trends for each series are also shown, together with their linear equations and explained variance. Gray vertical bars show positive (wet) CWAP values, and white vertical bars show negative (dry) CWAP values.

−0.36, significantly different from zero at the 95% level. Note that summer precipitation has no memory of the previous summer since the CWAP autocorrelation function at lag = −1 shows a null correlation. Thus, year-to-year summer precipitation variations are independent. Both the current summer precipitation and that of the previous summer (that which occurred during the previous growth–vintage cycle), contribute independently and inversely to similar fractions in the annual yield's variance. This is in agreement with the fact that bud differentiation and subsequent development–growth in grapevines have a 2-yr cycle (e.g., Mullins et al. 1992; Jones 2003).

Since the precipitation amounts during two consecutive summers prior to vintage contribute independently to the grape yield, it is possible to estimate a standard linear regression between detrended grape yield Y and detrended CWAP time series at both lag = 0 (DT CWAP lag = 0) and lag = −1 (DT CWAP lag = −1), as independent variables or predictors. The linear-regression analysis results in a determination coefficient $R^2 = 0.25$, significant at the 98% confidence level. Residuals point to the high degree of independence between the raw residuals and the multiregressional predictors, confirming the validity of the analysis (not shown). Thus, the combined effect of the precipitation during the two summers before the grape harvest explains about 25% of annual variance in yield.

This result can also be seen from a regional circulation perspective. Figure 4 shows the regression map between the yield index and PRWTR as given by the NCEP–NCAR reanalysis for both the summer of the year preceding the current cycle of grape growth and harvest (Fig. 4a) and the summer immediately before the harvest (Fig. 4b). PRWTR spatial anomalies patterns are similar for both summers, providing statistically significant reduced (enhanced) available moisture conditions over the CWA region, associated with high (low) grape yield. Other significant regions showing the "flip flop" relationship between yield and PRWTR are present over the eastern South Pacific, the South American convergence zone, and northeastern Brazil as well, suggesting possible links with large-scale circulation variability.

To verify whether the detrended CWAP index, which includes both liquid and solid precipitation, can furthermore adequately represent variations in the occurrence of hail events, it was correlated with the hail-damaged area SDG series for all of Mendoza's productive oases, for the period with available hail damage data (1994–2006; years $N = 13$). It ideally would have been better to have observed hail data, but no such data are available at a reasonable number of sites in the region with both adequate quality and sufficient temporal continuity. The
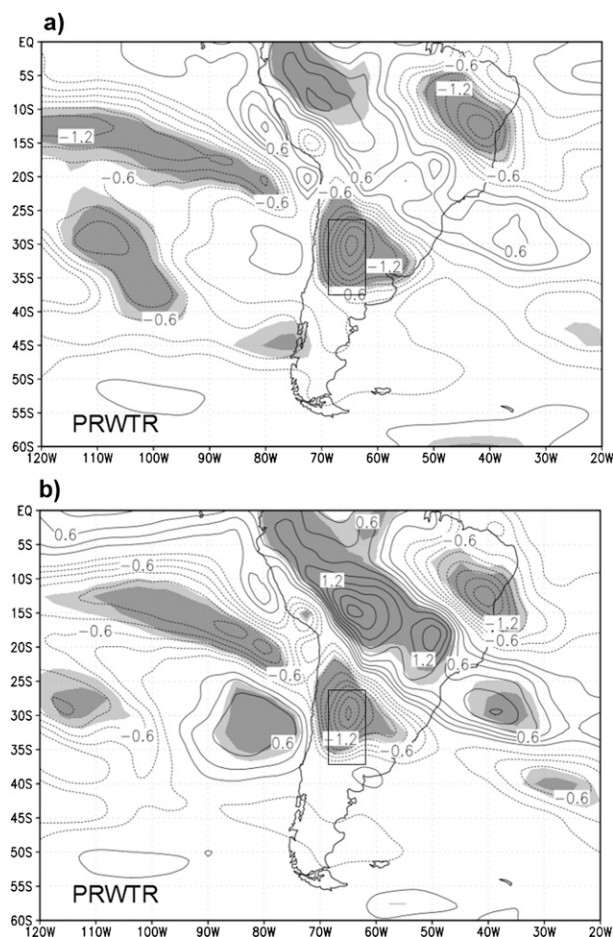

FIG. 4. PRWTR regressed on Mendoza's yield for (a) the summer during the year before harvest and (b) the summer immediately before the harvest. Units represent the fraction of PRWTR change (kg m^{-2}) per one standard deviation in grape yield. Significant values at the 90% (95%) confident level are shown in light-gray (gray) shading.

SDG series has a slightly negative trend in recent years that could be attributed to hail-damage prevention activities, such as sustained increases in the deployment of antihail nets over vineyards—in particular, premium ones. There is a significant linear relationship with CWAP, as given by the correlation coefficient $r = 0.56$, significant at the 95% level. This implies that precipitation changes can explain more than 30% of the variance in the hail-damaged area. Thus, summers, with more (less) precipitation are significantly associated with the occurrence of more (less) hail damage in vineyards.

Figure 5 shows the SDG series for the Eastern Zone oasis productive region only, which is the most convectively active area in Cuyo (Agosta et al. 1999), and the accumulated summer precipitation (PPPacum), between October and March. The period under analysis
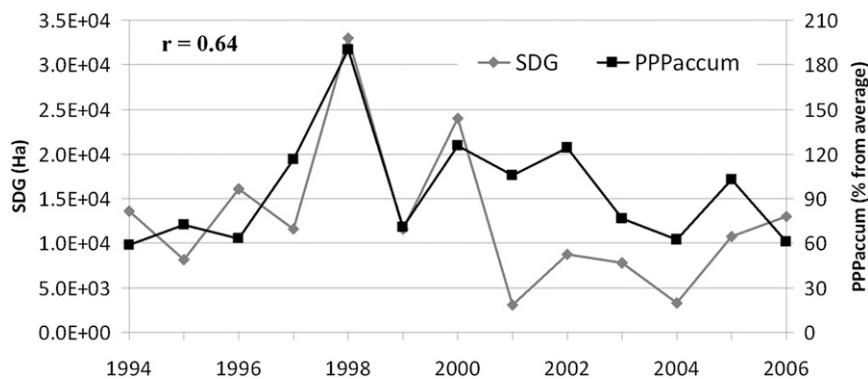
FIG. 5. Area damaged by hail in Mendoza's Eastern Zone oasis (SDG, ha), and October–March PPPacum, given as a percentage of the 1978–2008 summer average precipitation. The E on the SDG *y* axis indicates multiplication by 10 raised to the factor that follows it.

corresponds to the 1994–2006 harvests. The correlation coefficient between the two series is now 0.64, significant at the 98% level. Note that PPPacum shows enhanced variability prior to 2000 with a positive trend and reduced variability, and it shows a negative trend since, extending at least through 2006. The significant direct relationship between summer precipitation and hail damage in the eastern oasis is noteworthy and is slightly higher than in the analysis that uses the regional CWAP and total SDG.

The explanation for such relationships, as well as the link with severe weather, can be understood by analyzing plant state and response in the different phenological stages. Underlying causes that inversely couple summer precipitation with grape yield can be found in a number of processes. Yield can be affected, in the first place, by leaf area loss from defoliation that results from heavy-rain or hail events (i.e., direct damage) and, in the second place, by root suffocation resulting from prolonged flooding caused by water excesses during heavy summer rains (i.e., indirect damage; Gil and Pszczólkowski 2007). Nevertheless, the latter situation is a rare occurrence in Mendoza's arid-to-semiarid climate. At the same time, excess rainfall in general can have negative effects when it fosters the development of fungal diseases, mainly *Peronospora*, mildew, and *Botrytis*. These fungal diseases impact the photosynthetically active leaf surfaces and may affect the grapes as well, both as green berries and during the ripening stage (Gil and Pszczólkowski 2007). Thus, the current harvest's warm-season precipitation conditions can have a significant impact on yields.

Plant damage is relevant at any phenological stage, but it can have particularly significant consequences during the early development stages taking place during the summer of the preceding vintage. During this time, plant damage can cause the loss of full outbreaks, especially during flowering and cluster fruit setting. During these stages, severe storms and hail can dramatically reduce the amount of floral or fruit-setting clusters or leave injuries that result in a direct decrease in the plant production during the subsequent growth cycle (Sotés Ruiz 2011). Thus, humidity/precipitation conditions in the previous summer are also relevant, in agreement with the above results.

b. Low-frequency variability analysis

To understand further the observed links between CWAP and grape yield in the low-frequency range, time-period power analysis was carried out using wavelet techniques. Both yield and CWAP series time-period plots (Fig. 6a, top and bottom panels, respectively) show that the two variables have statistically significant signals (at least 90% significant) in the 6–8-yr period range. This period range remains statistically significant at least during the early 1990s for yield and throughout the 1990s and well into the 2000s for CWAP. Furthermore, yield appears to have significant variability in the 4-yr-period range in the mid-1980s and at periods close to 2 yr at higher frequencies during the late 1990s. This latter period range also appears in CWAP, although it is somewhat delayed in time and is less than 90% significant. Figure 6b shows the cross-wavelet transform, which provides information on the phase–time covariability between yield and CWAP. The grayscale shows where cross correlation is strong, and the arrows provide the phase difference between the two signals. Thus, in the 6–8-yr period range, the yield and CWAP are in antiphase during the first half of the 1990s. In the higher-frequency range, there would appear to be a significant cross correlation, 90° out of phase. As the wavelet squared coherence shows (Fig. 6c), however, the area where the higher-frequency perturbations occur in Fig. 6a does not coincide in time (i.e., around and after 1995), and hence the processes are not related. The wavelet analysis thus
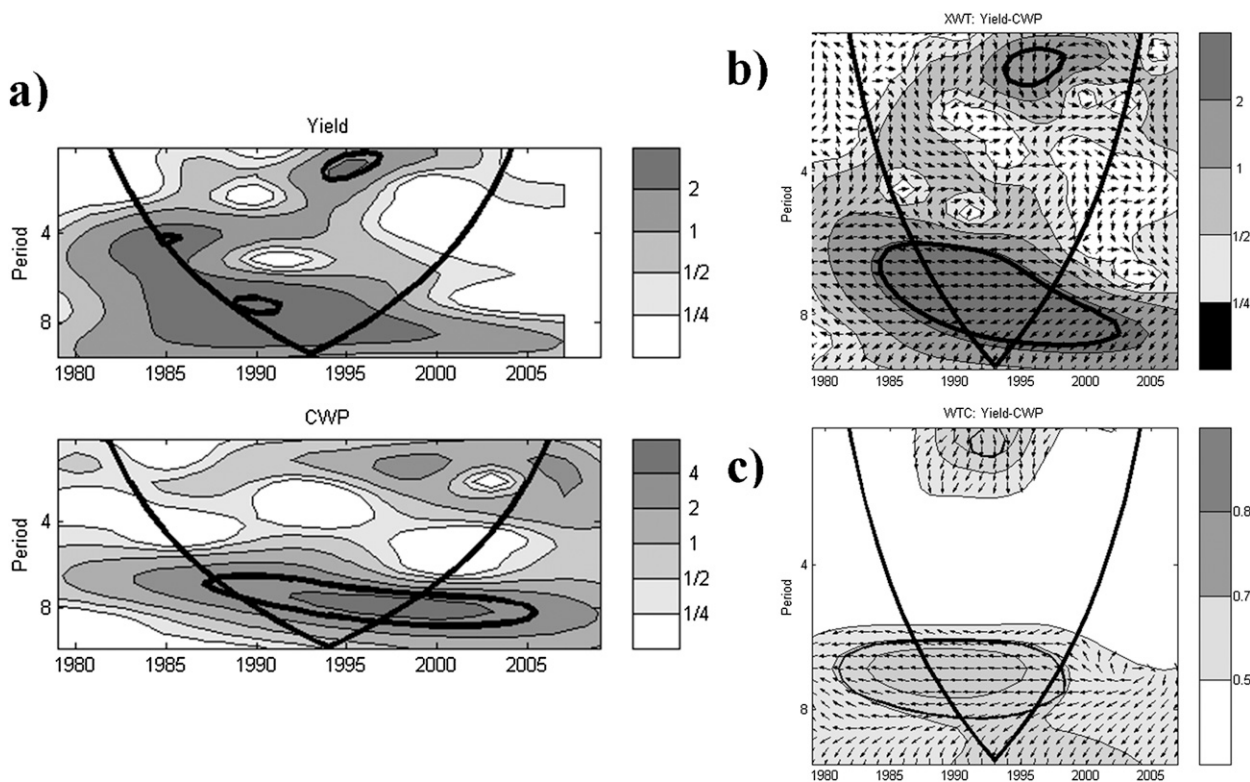
FIG. 6. Wavelet analysis of grape yield and CWAP time series showing the period–time space evolution of their variability. (a) Wavelet analysis plots of (top) grape yield and (bottom) CWAP. The thick lines highlight the areas where the variance is statistically significant, at least to the 90% level. (b) Cross-wavelet transform plot between grape yield and CWAP, showing their covariability. Arrows show the phase relationship between variables: in-phase behavior is shown by arrows that point to the right, and antiphase behavior is shown by arrows that point to the left. As before, the thick lines highlight significant areas. (c) Wavelet squared coherence plot that highlights the only significant relationship between grape yield and CWAP in the 6–9-yr range (see the text).

further points to an inverse relationship between grape yield and CWAP in the 6–8-yr period range during the first half of the 1990s.

The effect of precipitation associated with severe weather during the previous growing season together combined with the effect of preharvest summer precipitation and resulting water excesses leads to a smoothed modulation of the interannual variability in yield throughout the decade, effectively strengthening yield's decadal modulation. This kind of cause–effect process of precipitation upon grape yield, which is observed at decadal scales, probably could also be easily active throughout longer multidecadal scales such as the typical quasi-bidecadal oscillation that is present in earlier years in precipitation (Fig. 2).

c. Impacts of monthly temperature and precipitation variability

The relationship between yield and monthly precipitation and temperature, both maxima and minima, during the months preceding the annual grape harvest is another important feature of the climate–yield relationship. The

vintage period usually begins in mid-February and lasts until the end of April. The bulk of the grape harvest is carried out around March. In consequence, the annual grape cycle will be considered to extend, for current purposes, from May until March of the following year.

The correlations between detrended yield (YdT) and PPP are shown in Table 2. For months during the year of the preceding vintage (i.e., during the previous grape growth and harvest cycle: lag = −1), significant negative correlation values are obtained for January and March. During the current growing season (lag = 0), November and December are the only months with significant negative correlations with YdT. For the other summer months prior to the beginning of the harvest, correlations remain negative but are not significant. In all cases an inverse relationship between monthly precipitation and YdT is found, in agreement with CWAP results. The current, more time specific, analysis of the impact of the previous growing season's precipitation pinpoints January and March as the months with relevant precipitation impacts that contribute significantly to the CWAP lagged-correlation result. For the current vintage,

TABLE 2. Correlations and statistical significance values (in parentheses) between YdT and precipitation for months during which these are statistically significant.

	PPP previous Jan	PPP previous Mar	PPP Nov	PPP Dec
YdT	−0.59 (99%)	−0.35 (90%)	−0.36 (90%)	−0.49 (99%)

summer (December) precipitation appears to be the main contributor to the CWAP correlations.

The correlations between YdT and T_{min} (detrended monthly mean minimum temperature) or T_{max} (detrended monthly mean maximum temperature) are shown in Table 3. For T_{min}, a significant, positive correlation was found only for December. In contrast, T_{max} has significant and positive correlations during January of the previous growing season and during June, July, November, and December within the current growth period. The warm months within the growth period (i.e., November and December) appear to be decisive—in particular, the latter, which contributes to the yield both through T_{min} and T_{max}. If the monthly temperature range ($T_{max} - T_{min}$) is correlated with YdT, then correlations are significantly positive for June ($r = 0.36$), November ($r = 0.46$), and December ($r = 0.39$), again the latter two months being within the warm season. This suggests the need for significant diurnal thermal amplitudes at this time of the growth cycle.

Surface air temperature is a relevant variable, given its incidence upon cluster growth during different phenological stages. Both cluster growth and productivity depend on carbon uptake during photosynthesis and its subsequent processing, all of which is regulated by temperature (Sotés Ruiz 2011). Monthly T_{max} during November and December is important because it decisively influences berry setting and growth. This influence directly affects the final weight of the bunch and the total yield. Temperature range is important during these months because it primarily influences the fruit quality and the quantity and quality of polyphenolic compounds. The latter are relevant to the quality of the wine production, whereas the number of clusters obtained is not (e.g., Pszczólkowski et al. 2002; Santibáñez 2002; Rosier et al. 2004). Note also that thermal amplitude correlates with yield in November and December, because it primarily follows T_{max}, which is what really seems to be influencing the fruit development.

The T_{max} during June and July may influence cluster formation, both in quality and quantity. During these months the buds are in a state of ecolatency (or the ecodormition phase), and numerous authors (e.g., Kang et al. 1998; Wolf and Cook 1992; Wolf 2004; Ferguson et al. 2011) have noted the damage that very cold temperatures can have upon bud tissues during this development stage. Buds are capable of sprouting at this time, but they will not do so until the first warm spring temperatures trigger their opening and growth process and ensure the normal development of the new shoots (Pinto et al. 2009). The damage due to the very low winter temperatures will become evident in a deficient budburst in spring. Laboratory studies by Mills et al. (2006) evaluated the damage in the cane phloem and buds that can result from different winter conditions and showed that excessively low temperatures can result in significant damage and that enhanced humidity may increase injury. Note that in the Cuyo region the desert conditions result in monthly T_{max} with larger variance than that seen for T_{min} (i.e., 2° and 1.4°C, respectively) because of a greater sensitivity to cold-air intrusions during winter (June–August). The above positive correlations between T_{max} during winter months and YdT are thus in agreement with these results.

d. Large-scale tropospheric circulation and yield

Section 3c shows that local monthly precipitation and temperature have a direct impact on the interannual grape yield variability. In this section, tropospheric circulation variability associated with grape yield is analyzed to determine potential remote influences leading to such behavior. Tropical global SSTs are common forcing mechanisms of the extratropical tropospheric circulation—in particular, through the propagation of barotropic Rossby waves associated with SST-induced deep convection (Lau and Nath 1996).

An initial correlation analysis shows significant tropical SST association with yield, with correlations over 0.40 in the western equatorial Pacific (close to 5°N–5°S and 140°–160°E) during June, that is, during early winter when the vines are in dormancy state (Fig. 7a). Significant correlations over this equatorial ocean area can also be found beginning in March and maximizing in June. The June SST anomalies can be associated with anomalous deep convection over the area, to the northeast of Papua New Guinea, as inferred from the

TABLE 3. As in Table 2, but between YdT and T_{min} or T_{max}.

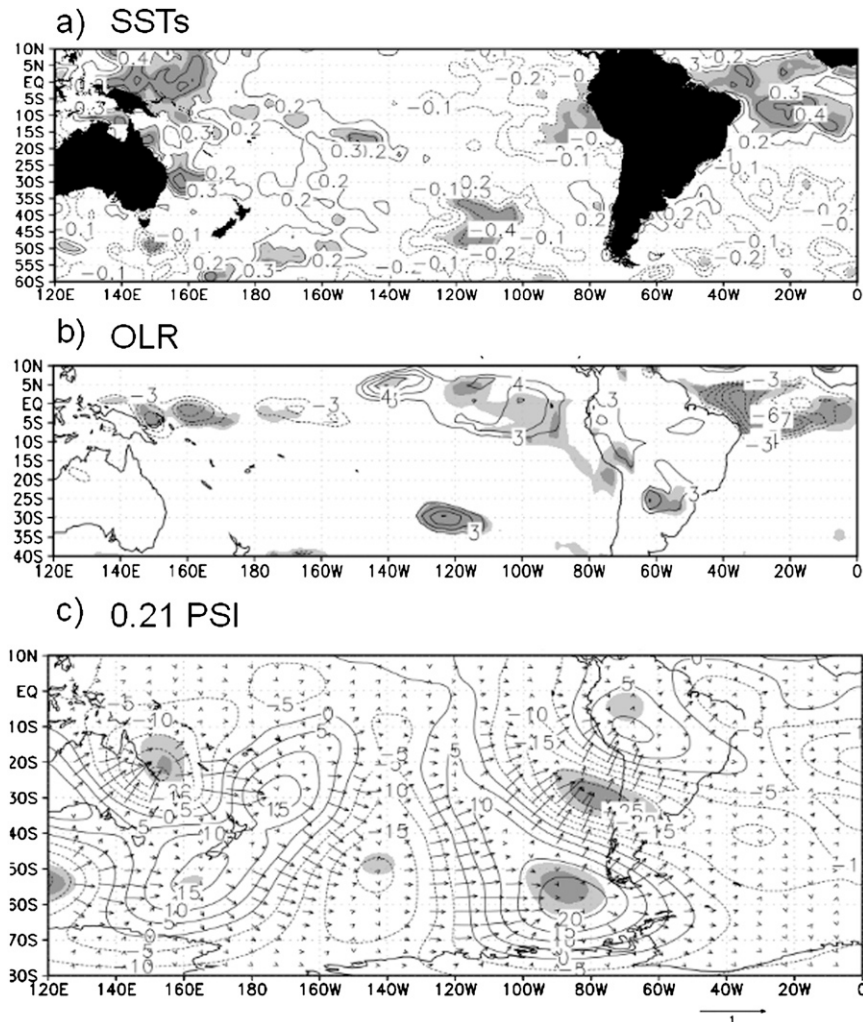|	T_{min} Dec	T_{max} previous Jan	T_{max} Jun	T_{max} Jul	T_{max} Nov	T_{max} Dec
YdT	0.37 (99%)	0.33 (90%)	0.42 (95%)	0.46 (98%)	0.51 (99%)	0.48 (99%)

FIG. 7. (a) Correlation map between June SSTs and the Mendoza grape yield. (b) OLR anomalies regressed on the grape yield (fraction of OLR change in watts per meter squared per one standard deviation in yield). (c) Upper-troposphere (sigma level 0.21) PSI anomalies regressed on the yield (fraction of PSI change in meters squared per second per one standard deviation in yield). The overlaid vector field shows the quasi-stationary wave activity flux $\mathbf{F}_s$ ($m^2\ s^{-2}$). Values that are significant at the 90% (95%) confident level are shown by light-gray (gray) shading.

significant and negative June OLR anomalies regressed upon yield (Fig. 7b), generating barotropic quasi-stationary wave propagation into the southern extratropics (Fig. 7c). Figure 7c also shows Plumb's $\mathbf{F}_s$ wave activity flux, which highlights the quasi-stationary wave propagation across the South Pacific from the source region in the western tropical Pacific. The anomalous wave pattern observed over South America in the lower troposphere favors the occurrence of surface warm (cold) advection over the CWA during winter (figures not shown), which is propitious for high (low) yields (see section 3b).

During subsequent winter and spring months, significant negative SST anomalies associated with yield

can be observed over the southeastern South Pacific (SEPAC), centered at 30°–45°S and 120°–100°W. In this region correlations are strong, with peak values above 0.50, which are maintained there over several months from July to November (Fig. 8a). These correlations, averaged over the area of maximum correlation between 35° and 45°S and between 115° and 105°W reach a maximum value in August. There is a strong and inverse relationship between the August SEPAC SST time series and yield that may serve as a potential tool for seasonal forecasting of annual yield in the next vintage in March–April. The prevalent negative seasonal SEPAC SSTs associated with grape yields during winter
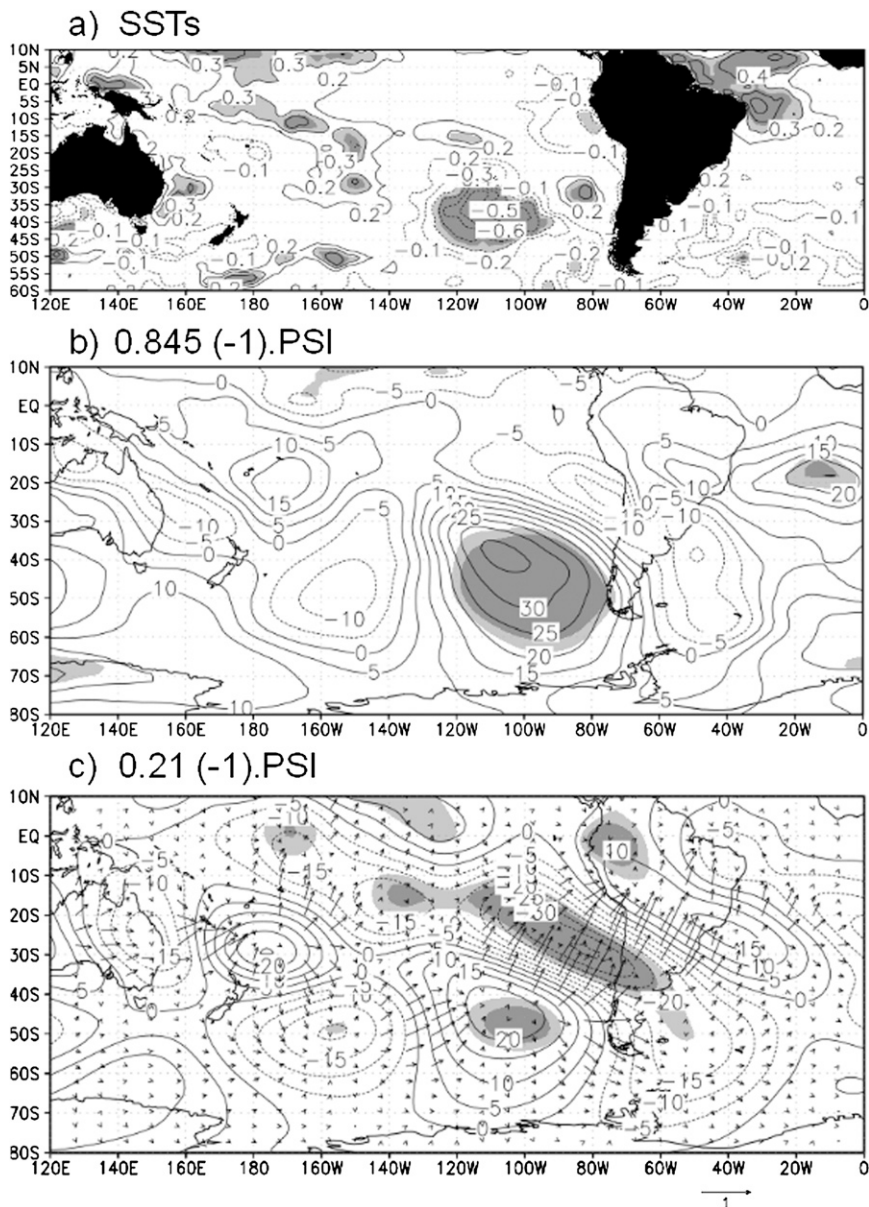
FIG. 8. (a) Correlation between yield and July–November mean SSTs. (b) June lower-troposphere (sigma level 0.85) PSI anomalies regressed upon SEPAC SST time series in August, multiplied by −1. (c) As in (b), but for the upper troposphere (sigma level 0.21). The values are the fractions of PSI change in meters squared per second per one standard deviation in yield. Overlaid vector field shows the quasi-stationary wave activity flux $\mathbf{F}_s$ (m^2 s^{-2}). Values that are significant at the 90% (95%) confident level are shown by light-gray (gray) shading.

and spring appear to respond to the early-winter quasi-stationary Rossby wave propagating from the equatorial western Pacific (Figs. 7a and 7c). Figures 8b and 8c show the lower- and upper-troposphere streamfunction fields, respectively, for June regressed upon the August SEPAC SST time series. Similar wave patterns (not shown) can be obtained for other regressions using spring SEPAC SST time series. Note the good agreement

between Figs. 7c and 8c. These results point out that early-winter (June) extratropical wave propagations as well as oceanic thermal inertia appear to be responsible for the generation of prevalent stationary midlatitude SEPAC SST anomalies during late winter and early spring, which in turn influence yield at the end of summer.

Thus, the question is how can these late winter–early spring SST anomalies over the SEPAC influence grape
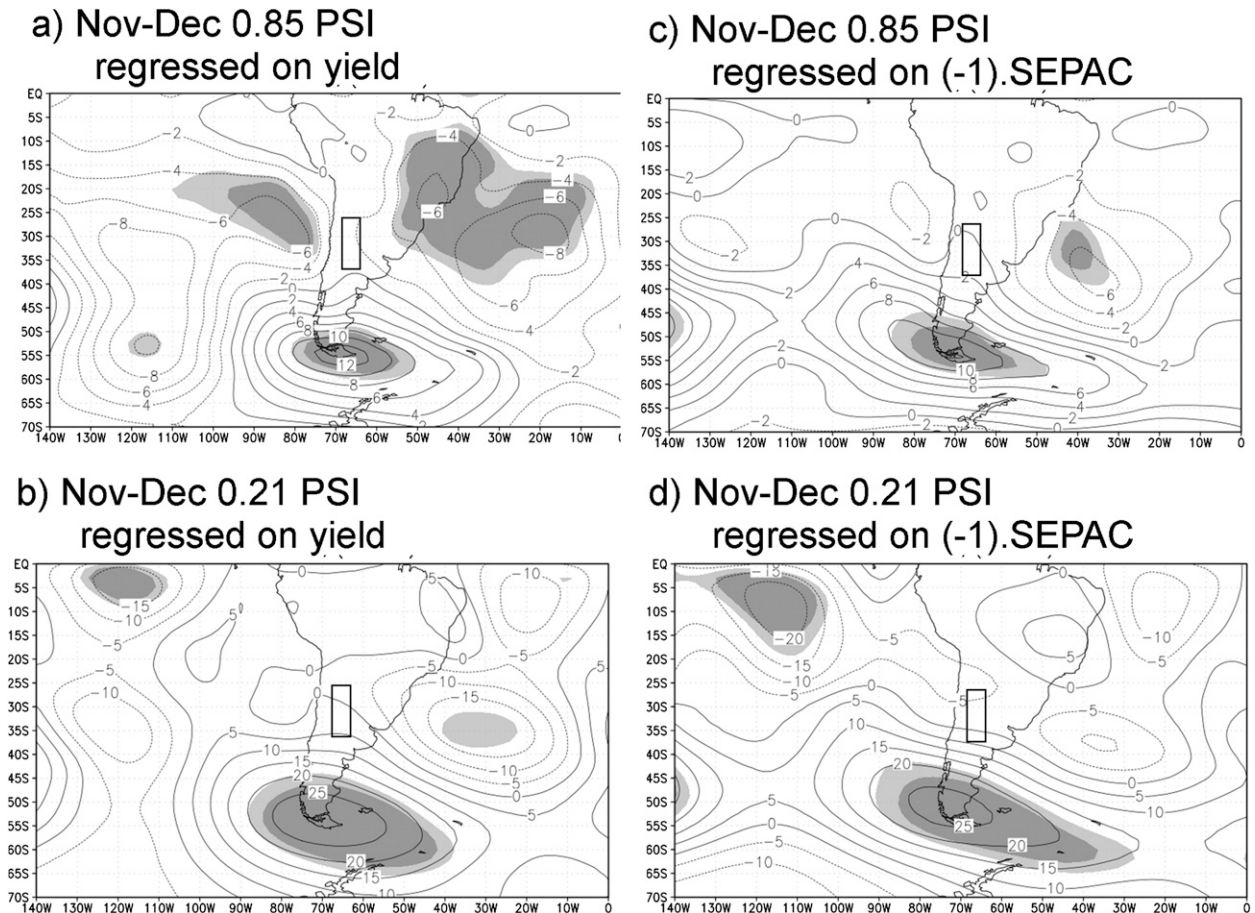
FIG. 9. November–December mean (a) lower-troposphere (sigma level 0.85) and (b) upper-troposphere (sigma level 0.21) PSI anomalies regressed on yield. Fractions of PSI change are in meters squared per second per one standard deviation in yield. (c),(d) As in (a) and (b), respectively, but for regression on August SEPAC SST (SEPAC). Values that are significant at the 90% (95%) confident level are shown by light-gray (gray) shading. The rectangles approximately indicate the location of the CWA region.

yield during the harvest of the following year? In section 3b, it has been established that local precipitation and temperature in November and December have a crucial influence on yield. Lower- and upper-troposphere streamfunction anomaly fields regressed on yield for the period of November–December are shown in Figs. 9a and 9b. Note that tropospheric circulation anomalies regressed upon the August SEPAC SST time series for the November–December yield have comparable anomaly patterns in the lower and upper troposphere (Figs. 9c and 9d) The regional barotropic tropospheric circulation anomalies in late spring associated with yields imply a weakening (enhancement) of the SAA together with weakening (strengthening) of the midlatitude westerlies for high (low) yields at the end of summer. The imposed tropospheric circulation anomalies, according to section 3b's results, lead to warmer (colder) airmass advection from the SAA toward the CWA, which can be deduced from the positive surface

air temperature anomalies over central Argentina in the regression map (Fig. 10a) and the advection of lower (higher) moisture masses from the midlatitude South Atlantic toward the CWA region, as can be observed by the negative PRWTR anomalies on the regression map (Fig. 10b). Therefore, the link between the SEPAC SST time series and yield must be found in the tropospheric circulation anomalies that are imposed in late spring/ early summer, resulting from the early-winter barotropic quasi-stationary wave propagation whose source in found in the western equatorial Pacific. These resulting circulation anomalies strongly influence vintage yields at the end of summer because of the phenological responses that were analyzed in section 3c.

e. Climate-based yield predictions

The current analysis has shown that for the climate variables under study there are potentially 11 predictors with a direct and local, quantifiable impact on Mendoza's
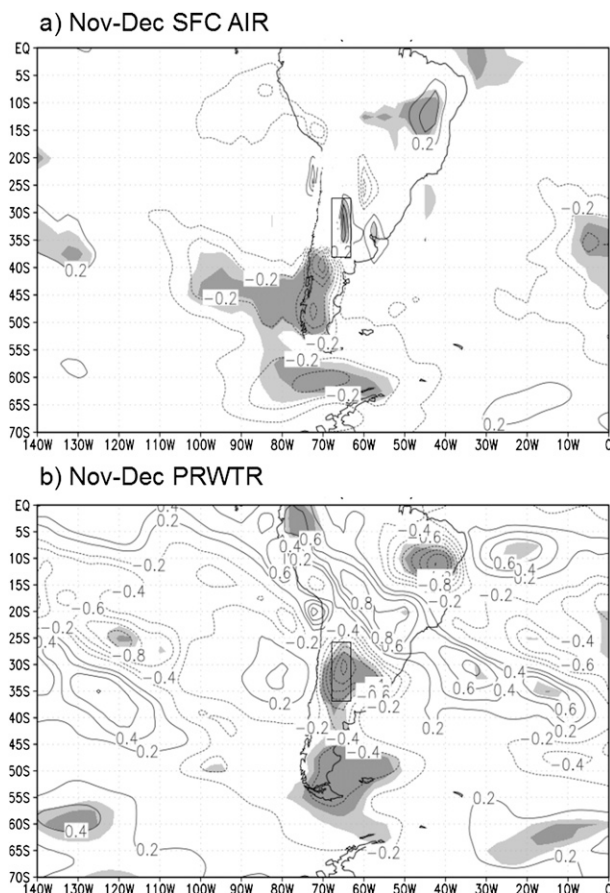
a) Nov-Dec SFC AIR

b) Nov-Dec PRWTR

FIG. 10. (a) November–December mean surface air temperature (SFC AIR) anomalies regressed on yield; values are in fraction of SFC Air change in kelvins per one standard deviation in yield. (b) As in (a), but for PRWTR. Values that are significant at the 90% (95%) confident level are shown by light-gray (gray) shading. The rectangles approximately indicate the location of the CWA region.

annual grape yield. These are precipitation during the months of November and December prior to vintage, precipitation during the January and March prior to the previous vintage, the maximum temperature during January of the previous year, the maximum temperatures during June and July (winter), the maximum temperatures during November and December (late spring and early summer), and the December minimum temperature. The potentiality of SEPAC SST time series in August as an external forcing predictor, adding quality to the model, can be further considered. Thus, a linear multiple regression using these variables can be obtained to describe their combined effect on the yield. When all 12 climate variables are considered together, the variance explained by the model is 76% ($r = 0.874$) at the 99% significance level.

On the other hand, the best possible fit, using a backward-stepwise selection method that is based on

an automatic procedure of variable inclusion/exclusion ($P \le 0.05$ and $P \ge 0.10$, respectively), is obtained when only three variables are considered: SEPAC SST in August, precipitation in January of the summer of the previous harvest, and the November maximum temperature of the current growth cycle. Figure 11 summarizes the statistical multilinear model. Figure 11a compares the observed yield time series with that predicted by the three-variable model. The explained variance is 63% ($r = 0.795$) at the 99% confidence level (Fig. 11b). Note that the model's β coefficients are 95% significant. The detrended normal probability plot (Fig. 11c) shows residuals from a normal distribution that are clustered around without a distinct pattern. This is evidence of the overall goodness of fit of this three-variable model. Furthermore, the scatterplots of the regression residuals versus predictors (Figs. 11d–f) do not show apparent problems with missing important predictors, as reflected by the fact that none of these plots shows a distinct pattern (Wilks 2006). In addition, the Durbin–Watson test yields a statistic $d = 2.174$ and a serial correlation of -0.17, which allows the rejection of the null hypothesis that the residuals are serially correlated at the 99% significance. This means that the residuals follow a stochastic process in time. The fact that August SEPAC SST is considered in the three-variable model, rather than other variables, confirms that, as discussed in section 3d, it is a good predictor of local climate variables in winter and spring, given its relationship with the observed regional circulation anomalies that are associated with yield.

Thus, the multiregression analysis shows that more than 60% of the interannual variability of the vintage yield depends on interannual climate variability. The almost 60% explained variance optimum predictive model for the grape harvest occurring in March–April can be applied by early December, at the beginning of the final berry development stages, to estimate harvest yields. The usefulness of this model is in that it requires only observed climatological information up to November. It would thus be possible to have a reasonable yield estimate taking into account climate and remote forcing variables 4 months before vintage.

4. Conclusions

Grape yield in Mendoza is significantly and inversely coupled throughout the sampled period to the summer precipitation in central-western Argentina. This could be due to two distinct climate processes that can affect grape yield every year, establishing distinct coupling processes: one process is due to extreme-precipitation events (i.e., hail damage on buds during the summer
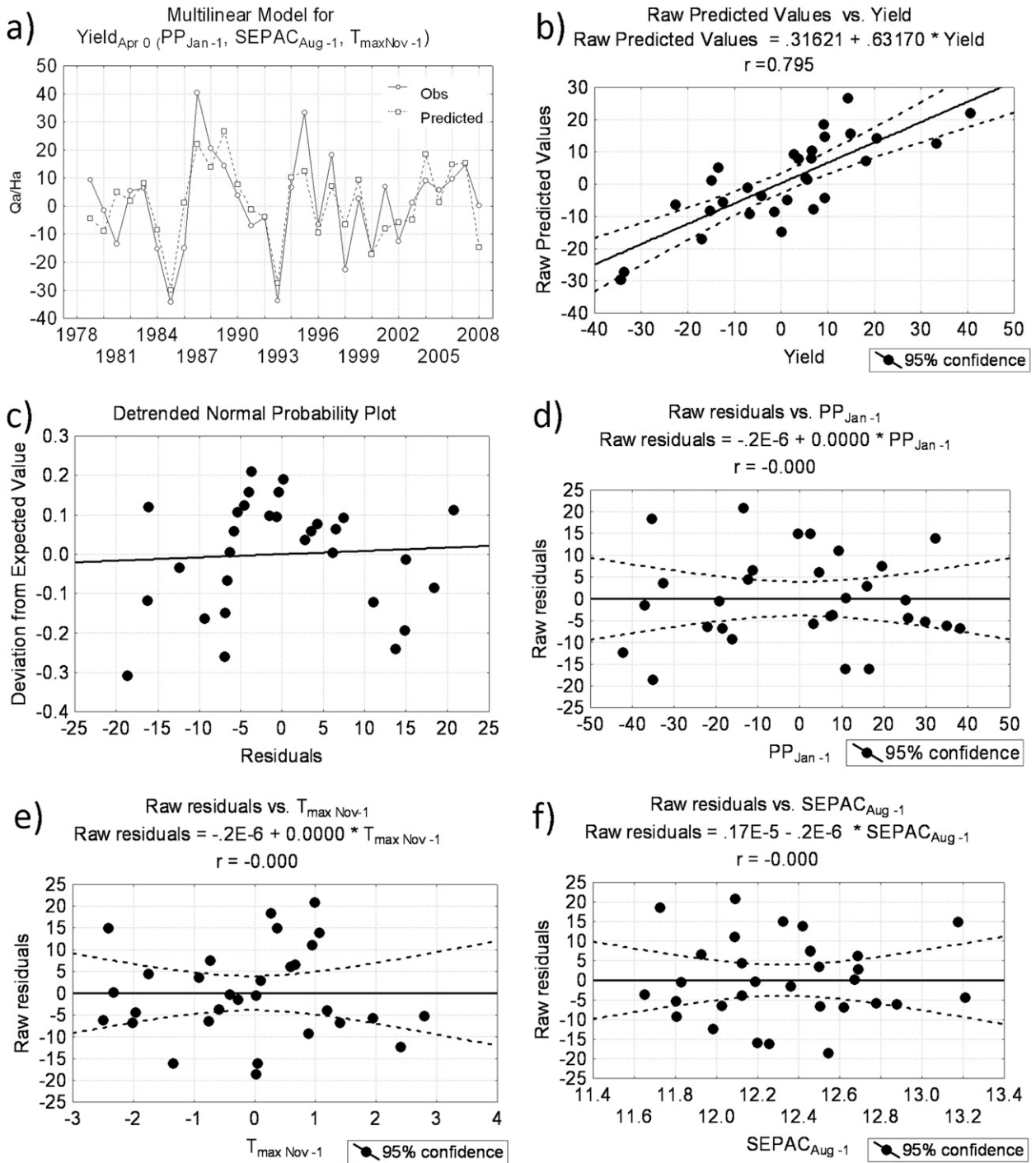
FIG. 11. Backward-stepwise model results, showing the three-variable model output. (a) Observed yield time series and model-predicted yield time series. (b) Linear relationship between raw predicted values and yield values. (c) Detrended normal probability plot showing residuals. This is evidence of the overall goodness of fit of this three-variable model. Scatterplots of raw residuals vs (d) January precipitation (PP_{Jan-1}) anomalies (mm), (e) November T_{max} ($T_{maxNov-1}$) anomalies (°C), and (f) August SEPAC SST ($SEPAC_{Aug-1}$; °C).

prior to the current growth–vintage cycle) and the other is damage caused by excess water in the crop (defoliation by intensity of rainfall, disease proliferation, etc.) during the summer months just before vintage. This

results in alternating periods of roughly 3–4 yr with high (low) grape yields due primarily to precipitation decadal variability. Because precipitation also shows multidecadal variability, the grape yield could in principle

also be affected over longer time scales. Likewise, given that precipitation in recent years has experienced an overall negative trend, it could be inferred that this trend could be responsible for part of the positive and significant trend in the province's yield, in addition to improvements resulting from the new varietal/clone selection and vineyard technologies implementation.

Distinct climate change scenarios, from coupled atmosphere–ocean general circulation models (GCM) using different greenhouse gas (GHG) thresholds, show an increase in summer precipitation within the CWA region by the end of the twenty-first century (Nuñez et al. 2008). For this reason if the low-frequency cause–effect process between precipitation and yield were to remain in the future, then negative grape yield anomalies would be expected. GCMs, however, are not currently capable of reproducing interdecadal teleconnection changes that can affect CWA summer precipitation, such as the climate change of 1976/77 (Agosta and Compagnucci 2012), since they are adjusted to a specific climate regime (Grimm et al. 2004). The analysis of grape yield evolution should be guided by both current GHGs scenarios and the understanding and monitoring of the dominant low-frequency climate basic states linked to precipitation in the CWA. Given the impacts of the Andes on Mendoza's climate and, in particular, upon the broad mountain valleys in which activity has been expanding in recent years, regional climate models with finer resolution are needed to better assess the future scenarios in the province and hence the potential impacts on vitiviniculture.

The analysis of the interannual precipitation variability within the annual cycle and its relationship with Mendoza's grape production has pinpointed during which months the two processes that negatively affect yield can have significant impacts. On the one hand, excess precipitation, which affects the flowering and setting of the clusters, is important during November and December. On the other hand, the impact of hail/severe weather upon this crop is such that it can generate partial or total damage/destruction of buds in entire parcels for the next harvest. This primarily occurs in January and March of the previous summer and partly during December of the current harvest, the latter directly affecting the clusters.

Furthermore, temperature during different phenological stages also plays an important role in the final yield. Results show that the maximum average monthly mean temperature in winter (June–July) along with the late spring (November) and early summer (December) during the growth cycle has an important and direct role in the yield in the subsequent harvest. These last two months show the greatest positive correlation, explaining approximately 25% of observed variance. The average maximum temperatures in November and December are important for the grape yield because of their importance in the setting and growth of berries. Although thermal amplitude is an essential parameter for determining cultivar fitness as used in various phenological indices, interannual variation of the average monthly thermal range, however, does not appear to play a role that is as well defined, but rather appears to follow the T_{max} behavior in relation to the crop in June and in November and December.

The analysis of the fields of various relevant atmospheric variables over the Pacific and Atlantic basins has highlighted possible climate processes that can affect CWA temperature and precipitation, with the consequences discussed above. A strong relationship between yield and late winter/early spring SSTs in the SEPAC region (30°–45°S, 120°–100°W) has been shown. SEPAC persistent anomalies can be linked to changes in tropical SSTs and deep convection over the eastern tropical Pacific during early winter. Indeed, this tropical SST anomaly and the associated convective activity become a source of quasi-stationary Rossby wave propagation into the extratropics, generating the observed seasonally persistent SEPAC SST anomalies. Last, the anomalies in the SAA, which influence the late spring and summer precipitation and temperatures over CWA, can themselves be traced back to the SEPAC SST anomalies. This relationship is so significant that the SEPAC SST in August is one of the three variables considered in the optimal best-fit model capable of predicting 60% of the yield's interannual variance, together with January precipitation and November T_{max}.

This analysis thus shows that Mendoza's regional climate variability and SST forcing can explain almost 60% of the interannual variance in the province's grape yield. Other climate/meteorological contributions to yield could arise when specific oases and/or varietals are considered because here the provincial bulk yield has been studied. Nevertheless, current results provide an observational basis necessary for improving the methods used to quantitatively assess yields at least 4 months before the March–April vintage period. These may also be useful in assessing the impacts of climate change scenarios upon the grape and wine industry.

REFERENCES

Agosta, E. A., and R. H. Compagnucci, 2008a: The 1976/77 austral summer climate transition effects on the atmospheric circulation and climate in southern South America. *J. Climate,* **21,** 4365–4383.

——, and ——, 2008b: Procesos atmosféricos/oceánicos de baja frecuencia sobre la cuenca sudoeste del Atlántico Sur y la variabilidad de la precipitación en el Centro-Oeste de Argentina (Low-frequency atmospheric/oceanic processes over the southwestern South Atlantic basin and precipitation variability in central-western Argentina). *Geoacta,* **33,** 11–22.

——, and M. A. Cavagnaro, 2010: Variaciones interanuales de la precipitación de verano y el rendimiento del cultivo de la vid en Mendoza (Interannual variations in summer precipitation and the grapevine yield in Mendoza). *Geoacta,* **35,** 1–11.

——, and R. H. Compagnucci, 2012: Central-west Argentina summer precipitation variability and atmospheric teleconnections. *J. Climate,* **25,** 1657–1677.

——, ——, and M. W. Vargas, 1999: Cambios en el régimen interanual de la precipitación estival en la región Centro-Oeste Argentina (Changes in the interannual precipitation regime in the central-western Argentina region). *Meteorológica,* **24,** 63–84.

Alexander, M., 2010: Extratropical air–sea interaction, sea surface temperature variability, and the Pacific decadal oscillation. *Climate Dynamics: Why Does Climate Vary?* D.-Z. Sun and F. Bryan, Eds., Amer. Geophys. Union, 123–148.

Barbero, N., C. Rössler, and P. Canziani, 2008: Cambio climático y viticultura: Variabilidad climática presente y futura y aptitud vitícola en 3 localidades de la Patagonia (Climate change and viticulture: Present and future climate variability and grapevine aptitude in three Patagonian localities). *Enología,* **5** (2), 8 pp. [Available online at http://www.revistaenologia.com/include/leer_pdf.php?id=121.]

Bond, N. A., J. E. Overland, M. Spillane, and P. Stabeno, 2003: Recent shifts in the state of the North Pacific. *Geophys. Res. Lett.,* **30,** 2183, doi:10.1029/2003Gl018597.

Compagnucci, R. H., E. A. Agosta, and M. W. Vargas, 2002: Climatic change and quasi-oscillations in central-west Argentina summer precipitation: Main features and coherent behaviour with southern African region. *Climate Dyn.,* **18,** 421–435.

Ebbesmeyer, C. C., D. R. Cayan, D. R. McLain, F. H. Nichols, D. H. Peterson, and T. Redmond, 1991: 1976 step in the Pacific climate: Forty environmental changes between 1968–1975 and 1977–1984. Proceedings of the Seventh Annual Pacific Climate PACLIM Workshop, California Dept. of Water Resources Interagency Ecological Studies Program Tech. Rep. 26, 115–126.

Ferguson, J. C., J. M. Tarara, L. J. Mills, G. G. Grove, and M. Keller, 2011: Dynamic thermal time model of cold hardiness for dormant grapevine buds. *Ann. Bot.,* **107,** 389–396.

Gil, G. F., and P. Pszczólkowski, 2007: *Viticultura: Fundamentos para Optimizar Producción y Calidad (Viticulture: Fundamentals for Optimizing Production and Quality).* Colección en Agricultura, Facultad de Agronomía e Ingeniería Forestal, Universidad Católica de Chile, 535 pp.

Grassi, B., G. Redaelli, P. O. Canziani, and G. Visconti, 2012: Effects of the PDO phase on the tropical belt width. *J. Climate,* **25,** 3282–3290.

Grifoni, D., M. Mancini, G. Maracchi, S. Orlandini, and G. Zipoli, 2006: Analysis of Italian wine quality using freely available meteorological information. *Amer. J. Enol. Vitic.,* **57,** 339–346.

Grimm, A. M., A. K. Sahai, and C. F. Ropelewski, 2004: Long-term variations in the performance of climate models. *Proc. XIII Congresso Brasileiro de Meteorologia,* Fortaleza, Brazil, Sociedade Brasileira de Meteorologia, 11 pp. [Available online at http://www.cbmet.com/cbm-files/22-eb14f6e8c5f7ff582618 ca27119b26c2.doc.]

Hall, A., and G. V. Jones, 2008: Effect of potential atmospheric warming on temperature-based indices describing Australian winegrape growing conditions. *Aust. J. Grape Wine Res.,* **15,** 97–119.

——, and ——, 2010: Spatial analysis of climate in winegrape-growing regions in Australia. *Aust. J. Grape Wine Res.,* **16,** 389–404.

Huang, H.-P., R. Seager, and Y. Kushnir, 2005: The 1976/77 transition in precipitation over the Americas and the influence of tropical sea surface temperature. *Climate Dyn.,* **24,** 721–740.

Jevrejeva, S., J. C. Moore, and A. Grinsted, 2003: Influence of the Arctic Oscillation and El Niño–Southern Oscillation (ENSO) on ice conditions in the Baltic Sea: The wavelet approach. *J. Geophys. Res.,* **108,** 4677, doi:10.1029/2003JD003417.

——, ——, P. L. Woodworth, and A. Grinsted, 2005: Influence of large scale atmospheric circulation on the European sea level: Results based on the wavelet transform method. *Tellus,* **57A,** 129–149.

Jones, G. V., 2003: Winegrape phenology. *Phenology: An Integrative Environmental Science,* M. D. Schwartz, Ed., Kluwer Academic, 525–539.

——, and R. Davis, 2000: Climate influences on grapevine phenology, grape composition, and wine production and quality for Bordeaux, France. *Amer. J. Enol. Vitic.,* **51,** 249–26.

——, M. White, O. Cooper, and K. Storchmann, 2005: Climate change and global wine quality. *Climatic Change,* **73,** 319–343.

Kang, S. K., H. Motosugi, K. Yonemori, and A. Sugiura, 1998: Supercooling characteristics of some deciduous fruit trees as related to water movement within the bud. *J. Hortic. Sci. Biotechnol.,* **73,** 165–172.

Kistler, R., and Coauthors, 2001: The NCEP–NCAR 50-Year Reanalysis: Monthly means CD-ROM and documentation. *Bull. Amer. Meteor. Soc.,* **82,** 247–268.

Lau, N.-C., and M. J. Nath, 1996: The role of the "atmospheric bridge" in linking tropical Pacific ENSO events to extratropical SST anomalies. *J. Climate,* **9,** 2036–2057.

Makra, L., B. Vitányi, A. Gál, J. Mika, I. Matyasovszky, and T. Hirsch, 2009: Wine quantity and quality variations in relation to climatic factors in the Tokaj (Hungary) winegrowing region. *Amer. J. Enol. Vitic.,* **60,** 312–321.

Mantua, N. J., S. R. Hare, Y. Zhang, J. M. Wallace, and R. C. Francis, 1997: A Pacific interdecadal climate oscillation with impacts on salmon production. *Bull. Amer. Meteor. Soc.,* **78,** 1069–1079.

Mills, L. J., J. C. Ferguson, and M. Keller, 2006: Cold-hardiness evaluation of grapevine buds and cane tissues. *Amer. J. Enol. Vitic.,* **57,** 194–200.

Mullins, M. G., A. Bouquet, and L. E. Williams, 1992: *Biology of the Grapevine.* Cambridge University Press, 239 pp.

Nuñez, M. N., S. Solman, and M. F. Cabré, 2008: Regional climate change experiments over southern South America. II: Climate change scenarios in the late twenty-first century. *Climate Dyn.,* **32,** 1081–1095.

Parry, M. L., O. F. Canziani, J. P. Palutikof, P. J. van der Linden, and C. E. Hanson, Eds., 2007b: *Fourth Assessment Report: Impacts, Adaptation and Vulnerability.* Cambridge University Press, 976 pp.

Pinto, M., W. Lira, H. Hugalde, and F. Pérez, 2009: Fisiología de la latencia de las yemas de la vid: Hipótesis actuals (Physiology of the latency of the yolks of the grapevine: Current hypotheses). BuscAgro–Directorio temático agropecuario y de ciencias afines, 16 pp. [Available online at http://www.gie.uchile.cl/pdf/Alvaro%20Pe%F1a/Fisiolog%EDa%20del%20receso%20de%20las%20yemas%20de%20vid.pdf.]

Plumb, R. A., 1985: On the three-dimensional propagation of stationary waves. *J. Atmos. Sci.,* **42,** 217–229.

Pszczólkowski, Ph., E. Alemparte, and M. I. Cárdenas, 2002: Aplicaciones del índice bioclimático de calidad de Fregoni simplificado en diversas áreas vitivinícolas de Chile: Proposición del uso de su evolución (Applications of Fregoni's simplified bioclimatic quality index in diverse grape-growing areas in Chile: Proposal for the use of its evolution). *Viticult. Enol. Prof.,* **82,** 27–39.

Rosier, J. P., E. Briguenti, E. Schuck, and V. Bonin, 2004: Comportamento da variedade Cabernet Sauvignon cultivada em vinhedos de altitude em São Joaquim-SC (Behavior of the Cabernet Sauvignon variety cultivated in vineyards of altitude in São Joaquim-SC). *Proc. XVIII Congresso Brasileiro de Fruticultura,* Florianópolis, Brazil, Sociedade Brasileira de Fruticultura, CD-ROM disk 1.

Saluzzi, M. E., 1992: Rol de la convección atmosférica como emergente, causante y regulador de las condiciones ambientales (Role of atmospheric convection as consequence, cause, and regulator of ambient conditions). Ph.D. thesis, University of Buenos Aires, 121 pp.

Santibáñez, F., 2002: Influencia del clima en la producción vitivinícola (Influence of climate in wine grape production). *Tópicos de Actualización en Viticultura y Enología (Current Topics in Viticulture and Enology),* Ph. Pszczólkowski, A. González, and G. Horman, Eds., G. Pontificia Universidad Católica de Chile, 21–36.

Solomon, S., D. Qin, M. Manning, M. Marquis, K. Averyt, M. M. B. Tignor, H. L. Miller Jr., and Z. Chen, Eds., 2007: *Climate Change 2007: The Physical Science Basis.* Cambridge University Press, 996 pp.

Sotés Ruiz, V., 2011: Avances en viticultura en el mundo (Advances in grape culture worldwide). *Rev. Bras. Frutic.,* **33,** doi:10.1590/S0100-29452011000500016.

Torrence, C., and G. P. Compo, 1998: A practical guide to wavelet analysis. *Bull. Amer. Meteor. Soc.,* **79,** 61–78.

——, and P. Webster, 1999: Interdecadal changes in the ESNO–monsoon system. *J. Climate,* **12,** 2679–2690.

Wilks, D. S., 2006: *Statistical Methods in the Atmospheric Sciences.* International Geophysics Series, Vol. 91, Academic Press, 627 pp.

Wolf, T. K., 2004: Crop yield effects on cold hardiness of 'Cabernet Sauvignon' dormant buds. *Acta Hortic.,* **640,** 177–187.

——, and M. K. Cook, 1992: Seasonal deacclimation patterns of three grape cultivars at constant, warm temperature. *Amer. J. Enol. Vitic.,* **43,** 171–179.

Zhang, Y., J. M. Wallace, and D. S. Battisti, 1997: ENSO-like interdecadal variability: 1900–93. *J. Climate,* **10,** 1004–1020.